

A Multiple Model SNR/RCS Likelihood Ratio Score for Radar-Based Feature-Aided Tracking

Benjamin J. Slocumb and Michael E. Klusman, III

Numerica Corporation, PO Box 271246, Ft. Collins, CO 82527, USA

ABSTRACT

Most approaches to data association in target tracking use a likelihood-ratio based score for measurement-to-track and track-to-track matching. The classical approach uses a likelihood ratio based on *kinematic* data. Feature-aided tracking uses *non-kinematic* data to produce an “auxiliary score” that augments the kinematic score. This paper develops a non-kinematic likelihood ratio score based on statistical models for the signal-to-noise (SNR) and radar cross section (RCS) for use in narrowband radar tracking. The formulation requires an estimate of the target mean RCS, and a key challenge is the tracking of the mean RCS through significant “jumps” due to aspect dependencies. A novel multiple model approach is used track through the RCS jumps. Three solution are developed: one based on an α -filter, a second based on the median filter, and the third based on an IMM filter with a median pre-filter. Simulation results are presented that show the effectiveness of the multiple model approach for tracking through RCS transitions due to aspect-angle changes.

Keywords: Feature-Aided Tracking, RCS Tracking, Multiple Model, Signal Score, Swerling Fluctuation

1. INTRODUCTION

Feature-aided tracking (FAT) is a technique where feature data are used to enhance the data association process in tracking. In the context of track-to-track correlation, the use of features is called feature-aided track correlation (FATC). Kinematic scores, based on distance metrics, are computed in the classical approach for determining the likelihood that a particular report should be associated to a given track. When feature data (e.g., RCS, intensity, length, etc.) are provided with the report, it is possible to compare it to a current estimate of that feature for the given track. Thus, association is enhanced when the report feature is similar to the track feature, and discouraged when it is different. The main challenge in FAT or FATC is to formulate a “score” (typically a likelihood ratio) that can be used in the association algorithm to quantify the similarity during association processing. Further, as the feature associated with a track changes over time, one needs a mechanism to “track” the changes. In the case of the RCS feature, the implementation of a dynamical model is difficult or prohibitive because of a lack of information about the target type and aspect-angle dependency.

A number of different approaches to FAT have been developed in the literature. Drummond^{1,2} describes a likelihood function for use in data association that incorporates the feature; errors in measuring the feature are assumed to be Gaussian (thus the likelihood involves a Chi-square parameter), and the feature mean is assumed to constant over time. Lerro and Bar-Shalom³ integrated an amplitude likelihood ratio into the standard PDAF association probabilities, which affected the association probabilities by favoring a high-amplitude measurement. Singer and Coursey⁴ developed a non-parametric FAT approach; this is a useful approach when nothing is known about the feature measurement density function. Agate and Sullivan⁵ provide a general derivation of measurement-to-track association hypotheses that include features and kinematic data; the work assumes the availability of a library of class-dependent feature measurement PDFs based on target classes and aspect angles (the main application envisioned is high range resolution radar). Nguyen⁶ *et al.* developed an approach that accumulates target classification information obtained from high range resolution radar to improve association scores. Lancaster, Blackman, and Taniguchi⁷ developed a technique using Dempster-Shafer methods for incorporating target classification data into the data association score.

In this paper, we address the specific problem of using radar signal features (SNR and RCS measurements from a narrowband radar) for augmenting the track score used in the data association problem. There are two main components to the work: (i) the signal score likelihood ratio formulation, and (ii) the RCS tracking technique. The general signal score likelihood ratio for data association used to augment the kinematic score is described in Blackman and Popoli.⁸ Likelihood ratios for specific RCS fluctuation models are derived following the work of Blackman and Fitzgerald.⁹ For the RCS tracking technique, we advance the multi-model RCS estimation approach in Ref. 9 that used a smoothing filter.

Other author information: Send correspondence to Email: bjslocumb@numerica.us, Telephone: 970-419-8343.

Report Documentation Page

Form Approved
OMB No. 0704-0188

Public reporting burden for the collection of information is estimated to average 1 hour per response, including the time for reviewing instructions, searching existing data sources, gathering and maintaining the data needed, and completing and reviewing the collection of information. Send comments regarding this burden estimate or any other aspect of this collection of information, including suggestions for reducing this burden, to Washington Headquarters Services, Directorate for Information Operations and Reports, 1215 Jefferson Davis Highway, Suite 1204, Arlington VA 22202-4302. Respondents should be aware that notwithstanding any other provision of law, no person shall be subject to a penalty for failing to comply with a collection of information if it does not display a currently valid OMB control number.

1. REPORT DATE 2005		2. REPORT TYPE		3. DATES COVERED 00-00-2005 to 00-00-2005	
4. TITLE AND SUBTITLE A Multiple Model SNR/RCS Likelihood Ration Score for Radar-Based Feature-Aided Tracking				5a. CONTRACT NUMBER	
				5b. GRANT NUMBER	
				5c. PROGRAM ELEMENT NUMBER	
6. AUTHOR(S)				5d. PROJECT NUMBER	
				5e. TASK NUMBER	
				5f. WORK UNIT NUMBER	
7. PERFORMING ORGANIZATION NAME(S) AND ADDRESS(ES) Numerica Corporation, PO Box 271246, Fort Collins, CO, 82527-1246				8. PERFORMING ORGANIZATION REPORT NUMBER	
9. SPONSORING/MONITORING AGENCY NAME(S) AND ADDRESS(ES)				10. SPONSOR/MONITOR'S ACRONYM(S)	
				11. SPONSOR/MONITOR'S REPORT NUMBER(S)	
12. DISTRIBUTION/AVAILABILITY STATEMENT Approved for public release; distribution unlimited					
13. SUPPLEMENTARY NOTES The original document contains color images.					
14. ABSTRACT see report					
15. SUBJECT TERMS					
16. SECURITY CLASSIFICATION OF:			17. LIMITATION OF ABSTRACT	18. NUMBER OF PAGES 12	19a. NAME OF RESPONSIBLE PERSON
a. REPORT unclassified	b. ABSTRACT unclassified	c. THIS PAGE unclassified			

We extend the work in two ways. First, we examine a variation on the approach by using median filters instead of the smoothing filter. Second, we formulate a new switching model approach that uses an IMM filter combined with a median filter. The median filter is ideal for processing data that has a “large tail” density (e.g., Swerling I).

This paper is organized as follows. In Section 2, we introduce some notation used throughout the paper. Section 3 develops the signal score for three different RCS fluctuation models: Swerling I, Swerling III, and log-normal. Section 4 develops three multi-model approaches for RCS estimation. Section 5 presents simulation results that compare the RCS estimation approaches. Finally, Section 6 summarizes the work.

2. NOTATION

For the convenience to the reader, we summarize here the notation used in the subsequent developments.

$L^{ij}(k)$ = the log-likelihood function for measurement- i , track- j , at time t_k .

$L_K^{ij}(k)$ = the kinematic portion of the log-likelihood function.

$L_S^{ij}(k)$ = the signal portion of the log-likelihood function.

\mathfrak{R}_k^j = the observed SNR of the j th measurement (linear units) at time t_k .

X_k^j = the RCS of the j th measurement (in m^2) at time t_k .

σ_k^j = the RCS of the j th measurement (in dBsm) at time t_k .

$\hat{\sigma}_{k|k-1}^i$ = the estimate of the target RCS associated with the i th track (in dBsm) at time t_k using data through time t_{k-1} .

3. SIGNAL SCORE MODEL

The track score (log-likelihood) for the i th track updated with the j th measurement at time t_k is described^{8,9} to be

$$L^{ij}(k) = L^i(k-1) + \Delta L^{ij}(k) \quad (1)$$

where

$$\Delta L^{ij}(k) = \begin{cases} \ln(1 - P_d), & \text{no track update} \\ \Delta L_K^{ij}(k) + \Delta L_S^{ij}(k), & \text{track update} \end{cases} \quad (2)$$

Here, $\Delta L_K^{ij}(k)$ is the incremental *kinematic* portion of the score update while $\Delta L_S^{ij}(k)$ is the incremental *signal* portion of the score update. The expression for the incremental signal score is given to be

$$\Delta L_S^{ij}(k) = \ln \left(\frac{P_d}{P_{fa}} \right) + \ln \left(\frac{p(\mathfrak{R}_k^j | H_1, \mathfrak{R}_k^j > \mathfrak{R}_{th})}{p(\mathfrak{R}_k^j | H_0, \mathfrak{R}_k^j > \mathfrak{R}_{th})} \right) \quad (3)$$

where \mathfrak{R}_k^j is defined to be the observed SNR of the j th measurement at time k . Here, $p(\mathfrak{R}_k^j | H_1, \mathfrak{R}_k^j > \mathfrak{R}_{th})$ is the probability density function (PDF) for the SNR given H_1 , the hypothesis that a signal is present, and given that the observed SNR exceeds the SNR detection threshold \mathfrak{R}_{th} . Also, $p(\mathfrak{R}_k^j | H_0, \mathfrak{R}_k^j > \mathfrak{R}_{th})$ is the PDF for the SNR conditioned on H_0 , the alternate hypothesis of noise only (or for clutter), and on the condition that the SNR exceeds the threshold. Since $p(\mathfrak{R}_k^j | H_1, \mathfrak{R}_k^j > \mathfrak{R}_{th}) = p(\mathfrak{R}_k^j | H_1) / P_d$, and $p(\mathfrak{R}_k^j | H_0, \mathfrak{R}_k^j > \mathfrak{R}_{th}) = p(\mathfrak{R}_k^j | H_0) / P_{fa}$, then (3) can be simplified to $\Delta L_S^{ij}(k) = \ln \left(p(\mathfrak{R}_k^j | H_1) / p(\mathfrak{R}_k^j | H_0) \right)$. However, the term $\ln(P_d / P_{fa})$ is often computed with $\Delta L_K^{ij}(k)$ when the score is implemented in software. Furthermore, nominal values for P_d and P_{fa} are frequently used. Thus, for this paper we will focus on the computation of the “augmenting signal score” that is defined by

$$L_{\mathfrak{R}}^{ij}(k) \triangleq \ln \left(\frac{p(\mathfrak{R}_k^j | H_1, \mathfrak{R}_k^j > \mathfrak{R}_{th})}{p(\mathfrak{R}_k^j | H_0, \mathfrak{R}_k^j > \mathfrak{R}_{th})} \right) \quad (4)$$

3.1. Score for the Swerling I Fluctuation Model

Four fluctuation models for the target RCS have been developed by Swerling.¹⁰ The Swerling I model is a scan-to-scan (slow) fluctuation model¹¹ that is appropriate for targets with many independent scattering points of which no single or few predominate. The Swerling II model is a pulse-to-pulse (fast) fluctuation model with the same RCS fluctuation density; the model is used in cases where the radar has a very low PRF, or for targets where very small changes in orientation cause large RCS changes.

The Swerling I density for the RCS is given by

$$p(X_k^j|H_1, \bar{X}) = \frac{1}{\bar{X}} \cdot \exp\left(-\frac{X_k^j}{\bar{X}}\right), \quad X_k^j \geq 0 \quad (5)$$

where \bar{X} is the mean RCS value. From this density for the RCS, the density for the SNR for a Swerling I model (for single pulse integration) can be shown to be exponentially distributed,⁸

$$p(\mathfrak{R}_k^j|H_1, \bar{\mathfrak{R}}) = \frac{1}{1 + \bar{\mathfrak{R}}} \cdot \exp\left(\frac{-\mathfrak{R}_k^j}{1 + \bar{\mathfrak{R}}}\right) \quad (6)$$

where $\bar{\mathfrak{R}}$ is the mean SNR. Here, H_1 is used to denote the hypothesis that the return is from a target and not noise.

Given that the return has exceeded the SNR threshold of \mathfrak{R}_{th} to be detected, then

$$p(\mathfrak{R}_k^j|H_1, \bar{\mathfrak{R}}, \mathfrak{R}_k^j > \mathfrak{R}_{th}) = \frac{1}{\bar{C}} \cdot \frac{1}{1 + \bar{\mathfrak{R}}} \cdot \exp\left(\frac{-\mathfrak{R}_k^j}{1 + \bar{\mathfrak{R}}}\right) \quad (7)$$

where the normalizing factor is given by $\bar{C} = \int_{\mathfrak{R}_{th}}^{\infty} p(\mathfrak{R}_k^j|H_1) d\mathfrak{R}_k^j = \exp(-\mathfrak{R}_{th}/(1 + \bar{\mathfrak{R}}))$. Thus,

$$p(\mathfrak{R}_k^j|H_1, \bar{\mathfrak{R}}, \mathfrak{R}_k^j > \mathfrak{R}_{th}) = \frac{1}{1 + \bar{\mathfrak{R}}} \cdot \exp\left(\frac{-\mathfrak{R}_k^j + \mathfrak{R}_{th}}{1 + \bar{\mathfrak{R}}}\right) \quad (8)$$

Meanwhile, the PDF for the case of noise only is given by $p(\mathfrak{R}_k^j|H_0) = \exp(-\mathfrak{R}_k^j)$. A clutter density (e.g., Weibull) could be used instead, if appropriate for the application. Given that the noise exceeded the SNR threshold of \mathfrak{R}_{th} to be detected, and since $\int_{\mathfrak{R}_{th}}^{\infty} \exp(\mathfrak{R}) d\mathfrak{R} = \exp(-\mathfrak{R}_{th})$, then the SNR density for the noise given it exceeded the threshold is given by $p(\mathfrak{R}_k^j|H_0, \mathfrak{R}_k^j > \mathfrak{R}_{th}) = \exp(-\mathfrak{R}_k^j + \mathfrak{R}_{th})$.

Using this density function, the augmenting signal score update becomes

$$L_{\mathfrak{R}}^{ij}(k) = \ln \left(\frac{p(\mathfrak{R}_k^j|H_1, \mathfrak{R}_k^j > \mathfrak{R}_{th})}{p(\mathfrak{R}_k^j|H_0, \mathfrak{R}_k^j > \mathfrak{R}_{th})} \right) = -\ln(1 + \bar{\mathfrak{R}}^i) + \frac{(\mathfrak{R}_k^j - \mathfrak{R}_{th})\bar{\mathfrak{R}}^i}{1 + \bar{\mathfrak{R}}^i} \quad (9)$$

To compute this score, one needs to know $\bar{\mathfrak{R}}^i$, the mean SNR for the i th target. This can be computed as $\bar{\mathfrak{R}}^i = C_0 \bar{X}^i$, where \bar{X}^i is the mean RCS and C_0 is constant that is a known function of radar parameters (power, wavelength, range, etc.). In general, \bar{X}^i is unknown, but this can be estimated as we will discuss in Section 4. The challenge is that the RCS can suddenly change based on the aspect angle to the target.

3.2. Score for the Swerling III Fluctuation Model

The Swerling III model for target RCS is a scan-to-scan (slow) fluctuation model¹¹ that is appropriate for targets that have one main scattering element that predominates together with many smaller independent scattering elements. This model is sometimes assumed for radars with lower frequencies (e.g., below 1.0 GHz) and for small streamlined aircraft targets. The Swerling IV model is a pulse-to-pulse (fast) fluctuation model that uses the same RCS density.

The PDF for the Swerling III RCS is given by

$$p(X_k^j|H_1, \bar{X}) = \frac{4X}{\bar{X}^2} \cdot \exp\left(\frac{-2X}{\bar{X}}\right), \quad X \geq 0 \quad (10)$$

where \bar{X} is the mean RCS. The corresponding pdf⁸ of the observed SNR for a Swerling III target (for single pulse integration) is given by

$$p(\mathfrak{R}_k^j|H_1, \bar{\mathfrak{R}}) = \left(1 + \frac{\mathfrak{R}_k^j}{1 + 2/\bar{\mathfrak{R}}}\right) \cdot \frac{1}{(1 + \bar{\mathfrak{R}}/2)^2} \cdot \exp\left(\frac{-\mathfrak{R}_k^j}{1 + \bar{\mathfrak{R}}/2}\right) = \frac{4(2 + \bar{\mathfrak{R}} + \bar{\mathfrak{R}}\mathfrak{R}_k^j)}{(2 + \bar{\mathfrak{R}})^2} \exp\left(\frac{-2\mathfrak{R}_k^j}{2 + \bar{\mathfrak{R}}}\right) \quad (11)$$

where the mean SNR is $\bar{\mathfrak{R}}$. Given that the return was detected, then the SNR must be greater than the threshold* \mathfrak{R}_{th} . The normalization component is derived as

$$\int_{\mathfrak{R}_{th}}^{\infty} p(\mathfrak{R}_k^j|H_1, \bar{\mathfrak{R}}) d\mathfrak{R}_k^j = \frac{(\bar{\mathfrak{R}}^2 + 4\bar{\mathfrak{R}} + 2\bar{\mathfrak{R}}\mathfrak{R}_{th} + 4)}{(2 + \bar{\mathfrak{R}})^2} \exp\left(\frac{-2\mathfrak{R}_{th}}{2 + \bar{\mathfrak{R}}}\right) \quad (12)$$

Therefore, the density for the SNR given it exceeds the threshold is

$$p(\mathfrak{R}_k^j|H_1, \bar{\mathfrak{R}}, \mathfrak{R}_k^j > \mathfrak{R}_{th}) = \frac{4(2 + \bar{\mathfrak{R}} + \bar{\mathfrak{R}}\mathfrak{R}_k^j)}{(2 + \bar{\mathfrak{R}})(\bar{\mathfrak{R}}^2 + 4\bar{\mathfrak{R}} + 2\bar{\mathfrak{R}}\mathfrak{R}_{th} + 4)} \exp\left(\frac{-2(\mathfrak{R}_k^j - \mathfrak{R}_{th})}{2 + \bar{\mathfrak{R}}}\right) \quad (13)$$

To compute the denominator of the log-likelihood ratio, we again use the noise density given that the SNR is above the detection threshold, $p(\mathfrak{R}_k^j|H_0, \mathfrak{R}_k^j > \mathfrak{R}_{th}) = \exp(-\mathfrak{R}_k^j + \mathfrak{R}_{th})$.

Using these density functions, the augmenting signal score becomes

$$L_{\mathfrak{R}}^{ij}(k) = \ln\left(\frac{p(\mathfrak{R}_k^j|H_1, \bar{\mathfrak{R}}^i, \mathfrak{R}_k^j > \mathfrak{R}_{th})}{p(\mathfrak{R}_k^j|H_0, \mathfrak{R}_k^j > \mathfrak{R}_{th})}\right) = \ln\left(\frac{4(2 + \bar{\mathfrak{R}}^i + \bar{\mathfrak{R}}^i\mathfrak{R}_k^j)}{(2 + \bar{\mathfrak{R}}^i)(\bar{\mathfrak{R}}^i{}^2 + 4\bar{\mathfrak{R}}^i + 2\bar{\mathfrak{R}}^i\mathfrak{R}_{th} + 4)}\right) + \frac{\bar{\mathfrak{R}}^i(\mathfrak{R}_k^j - \mathfrak{R}_{th})}{2 + \bar{\mathfrak{R}}^i} \quad (14)$$

Again, to compute this score one needs to know $\bar{\mathfrak{R}}^i$. An estimate can be derived if one tracks the mean RCS of the target. Sudden changes in RCS based on the target aspect angle present the challenge in estimating \bar{X}^i .

3.3. Score for the Log-Normal Fluctuation Model

Another accepted RCS fluctuation model is the log-normal distribution,¹¹

$$p(X_k^j|H_1, \bar{X}, \varsigma) = \frac{1}{\sqrt{2\pi\varsigma}X_k^j} \exp\left(-\frac{1}{2\varsigma^2} \left[\ln\left(X_k^j/\bar{X}\right)\right]^2\right) \quad (15)$$

where \bar{X} is the *median value* of X , and ς is the standard deviation of $\ln(X/\bar{X})$. Apparently, this model can approximate the radar cross section of some satellites, cylinders, plates, and arrays. With a change of variables, $\sigma = \ln(X)$, then we would find that the PDF for σ is

$$p(\sigma_k^j|H_1, \bar{\sigma}, \varsigma^2) = \frac{1}{\sqrt{2\pi\varsigma}} \exp\left(\frac{-(\sigma_k^j - \bar{\sigma})^2}{2\varsigma^2}\right) \quad (16)$$

where $\bar{\sigma} = \ln(\bar{X})$. Since we typically report the RCS in units of dBsm, then we can simply use (16) with $\sigma_k^j = 10 \log(X_k^j)$ if we define ς to be the standard deviation of $10 \log(X/\bar{X})$ instead. This model was adopted in the report by Blackman⁹ for forming a signal score log-likelihood ratio.

The SNR, \mathfrak{R}_k^j , and the radar cross section, X_k^j (m² units) or σ_k^j (dBsm units), can be related in terms of the known radar parameters C_0 ,

$$\mathfrak{R}_k^j = C_0 \cdot X_k^j = C_0 \cdot \exp\left(\frac{\sigma_k^j}{10 \log(e)}\right) \triangleq f(\sigma_k^j) \quad (17)$$

*Note that the ‘‘signal detection threshold’’ is typically given as $\gamma_{th} = \mathfrak{R}_{th} \cdot P_n$, where P_n is the noise power.

Now, given an assumed probability density for the RCS in (16), we can transform through the function $\mathfrak{R}_k^j = f(\sigma_k^j)$ which is defined in (17) to obtain the probability density function for the SNR,

$$p_{\mathfrak{R}} \left(\mathfrak{R}_k^j \mid H_1, \bar{\sigma}, \varsigma \right) = p_{\sigma} \left(f^{-1}(\mathfrak{R}_k^j) \mid H_1, \bar{\sigma}, \varsigma^2 \right) \left| \frac{\partial f^{-1}(y)}{\partial y} \right|_{y=\mathfrak{R}_k^j} \quad (18)$$

Applying the transformation, we obtain the following density function for the SNR of the j th measurement (given a signal is present),

$$p(\mathfrak{R}_k^j \mid H_1, \bar{\sigma}, \varsigma) = \frac{10 \log_{10}(e)}{\mathfrak{R}_k^j} p(\sigma_k^j \mid H_1, \bar{\sigma}, \varsigma^2) \quad (19)$$

where $\sigma_k^j = f^{-1}(\mathfrak{R}_k^j) = 10 \log(e) \ln(\mathfrak{R}_k^j / C_0)$. Then, assuming the density for the RCS from (16), the SNR density simplifies to

$$p(\mathfrak{R}_k^j \mid H_1, \bar{\sigma}, \varsigma) = \frac{10 \log_{10}(e)}{\sqrt{2\pi\varsigma} \mathfrak{R}_k^j} \exp \left(-\frac{(\sigma_k^j - \bar{\sigma})^2}{2\varsigma^2} \right) \quad (20)$$

Since the detection is only obtained when the return exceeds the threshold \mathfrak{R}_{th} , we must scale the density by a constant,

$$\bar{C} \triangleq \int_{\mathfrak{R}_{th}}^{\infty} p(\mathfrak{R}_k^j \mid H_1, \bar{\sigma}, \varsigma^2) = \frac{1}{2} \left(1 + \operatorname{erf} \left(\frac{\sqrt{2}(\bar{\sigma} - \sigma_{th})}{2\varsigma} \right) \right) \quad (21)$$

where $\sigma_{th} = 10 \log(e) \ln(\mathfrak{R}_{th} / C_0)$. Therefore, the pdf for the SNR, given the return exceeded the threshold, is given by

$$p(\mathfrak{R}_k^j \mid H_1, \bar{\sigma}, \varsigma, \mathfrak{R}_k^j > \mathfrak{R}_{th}) = \frac{10 \log_{10}(e)}{\sqrt{2\pi\varsigma} \mathfrak{R}_k^j \bar{C}} \exp \left(-\frac{(\sigma_k^j - \bar{\sigma})^2}{2\varsigma^2} \right) \quad (22)$$

The null hypothesis density, given that the return exceeds the required signal-to-noise \mathfrak{R}_{th} , is $p(\mathfrak{R}_k^j \mid H_0, \mathfrak{R}_k^j > \mathfrak{R}_{th}) = \exp(-\mathfrak{R}_k^j + \mathfrak{R}_{th})$.

Inserting the density functions into the likelihood ratio gives us the augmenting signal score,

$$L_{\mathfrak{R}}^j(k) = \mathfrak{R}_k^j - \mathfrak{R}_{th} - \ln \mathfrak{R}_k^j - \ln \bar{C}^i + \ln(10 \log_{10}(e)) - \ln(\sqrt{2\pi\varsigma^i}) - \frac{(\sigma_k^j - \bar{\sigma}^i)^2}{2(\varsigma^i)^2} \quad (23)$$

Implementation of this solution requires the knowledge of \mathfrak{R}_{th} , \bar{C}^i , $\bar{\sigma}^i$, and ς^i . The first two come from radar system parameters[†]. We note that for most cases that $\ln(\bar{C}^i) \approx 0$, and therefore can effectively be ignored. The median RCS, $\bar{\sigma}^i$, has to be estimated since it is a target-dependent parameter. The variance $(\varsigma^i)^2$ is an RCS fluctuation model parameter; it could be assumed or estimated.

3.4. Comparisons of RCS and Median Filtered RCS Fluctuation Distributions

Several of the RCS filtering techniques developed in Section 4 make use of median filters. Thus, it is useful to relate the median value to the mean value of the Swerling distributions discussed above. To find the relationship, we integrate the Swerling density as follows, $y = \int_0^T p(X \mid H_1, \bar{X}) dX$. Then the median is $X_{\text{median}} = T$ such that $y = 0.5$. Solving this expression for the Swerling I RCS distribution, we find that $X_{\text{median}} = 1.4427 \times \bar{X}$. For the Swerling III distribution, we find that $X_{\text{median}} = 1.1916 \times \bar{X}$.

To understand the effect of median filtering on RCS data, we performed simulations of the median filtered RCS distributions (window size $w = 3$) for the Swerling I and Swerling III models. Based on a comparison of plots, the median filtered Swerling I RCS data closely matches the distribution for the log-normal distribution with a standard deviation of 3.0 dBsm. For Swerling III, the median filtered distribution closely matches the log-normal distribution, but here the standard deviation of the log-normal is 2.0 dBsm instead. Thus, one can conclude that median-filtered Swerling I and III RCS data has a distribution that approximates a log-normal distribution; this characteristic is advantageous when developing RCS filtering methods that use a median pre-filter.

[†] If the signal scoring is done remotely from the radar, then it is possible that the tracker may not have access to these parameters. The use of approximations may be necessary.

4. MULTIPLE MODEL RCS ESTIMATION

To compute three signal score expressions in (9), (14), and (23) requires and estimate for \mathfrak{R}^i or equivalently \bar{X}^i . Since RCS is a target-dependent variable, and SNR is a function of range and the instantaneous radar parameters, it makes sense that one should track the RCS of the target. From this estimate one can infer the predicted SNR. In this section, we describe three methods for predicting the target mean RCS using tracking methods. The preferred approach would be to have a catalog of all target RCS patterns and to “look up” the mean RCS based on a target type estimate and an aspect angle estimate. This is effectively a target classification problem, which has been treated as an Hidden Markov Model (HMM) problem in the literature.^{12,13} However, maintaining a catalog of all target types is often prohibitive, therefore our approach is to attempt to estimate the mean (or median) RCS based on recent measurements and using *no a priori* data about the target. The difficulty in estimating the RCS is that the mean RCS can rapidly change as the aspect angle to the target changes. For example, large returns can be obtained when directly aligned with the nose section of an aircraft, while smaller returns can be obtained at angles slightly off the nose. To handle these “jumps” in the RCS as the aspect angle changes, three multiple-model estimators have been developed. The three approaches are compared in Section 5.

4.1. Two-Model RCS Estimator with α -Filters

An approach described in Ref. 9 uses a Bayesian model to allow for good “smoothing” for stable RCS conditions and “jumps” when rapid RCS changes occur due to aspect-angle dependencies. Two estimates (short- and long-term) are obtained using two α -filters. Define σ_k^j to be the RCS measurement associated with the j th measurement (in dBsm units). Let $\hat{\sigma}_{k|k-1}^{i_1}$ and $\hat{\sigma}_{k|k-1}^{i_2}$ be the short-term and long-term estimates of the RCS[‡], respectively, associated with the i th track. Log-normal probability densities are assumed for the two RCS model hypotheses,

$$p(\sigma_k^j|h_1) = \frac{1}{\sqrt{2\pi\zeta_1}} \cdot \exp\left(\frac{-(\sigma_k^j - \hat{\sigma}_{k|k-1}^{i_1})^2}{2\zeta_1^2}\right), \quad p(\sigma_k^j|h_2) = \frac{1}{\sqrt{2\pi\zeta_2}} \cdot \exp\left(\frac{-(\sigma_k^j - \hat{\sigma}_{k|k-1}^{i_2})^2}{2\zeta_2^2}\right) \quad (24)$$

Here, hypothesis h_1 corresponds to the short-term model and hypothesis h_2 corresponds to the long-term model. Also, ζ_1^2 and ζ_2^2 are variances associated with the short- and long-term RCS models. Using Bayes’ theorem, the *a priori* probabilities at time t_k are

$$p_k(h_1) = \frac{p(\sigma_k^j|h_1)p_{k-1}(h_1)}{p(\sigma_k^j|h_1)p_{k-1}(h_1) + p(\sigma_k^j|h_2)p_{k-1}(h_2)}, \quad p_k(h_2) = \frac{p(\sigma_k^j|h_2)p_{k-1}(h_2)}{p(\sigma_k^j|h_1)p_{k-1}(h_1) + p(\sigma_k^j|h_2)p_{k-1}(h_2)} \quad (25)$$

where $p_k(h_n)$ is the computed probability for filter mode h_n using data up to time t_k . Initial prior mode probabilities are set to be $p_0(h_1) = p_0(h_2) = 0.5$. Note that it is possible that $p(\sigma_k^j|h_1) \rightarrow 0$ or $p(\sigma_k^j|h_2) \rightarrow 0$, hence in the calculation of (25) one must place a floor value $p_{min} \approx 0.01$ on the mode probabilities; otherwise, the filter could “get stuck” in one mode.

The short and long-term estimates of the RCS are computed using an α -filter with all the data up to time t_k ,

$$\hat{\sigma}_{k|k}^{i_1} = (1 - \alpha_1)\hat{\sigma}_{k|k-1}^{i_1} + \alpha_1\sigma_k^j, \quad \hat{\sigma}_{k|k}^{i_2} = (1 - \alpha_2)\hat{\sigma}_{k|k-1}^{i_2} + \alpha_2\sigma_k^j \quad (26)$$

where

$$\alpha_1 = \max(1 - \exp(-T_{k-1}/\tau_1), \alpha_1^{\min}), \quad \alpha_2 = \max(1 - \exp(-T_{k-1}/\tau_2), \alpha_2^{\min}) \quad (27)$$

and $T_{k-1} = t_k - t_{k-1}$ is the sampling interval (time since last update of the i th track). The time constants τ_1 and τ_2 are user-defined parameters that should be selected based on the aspect-angle change rate of the target (target range and velocity) and the sensor update rate. Also, it can be useful to place upper and lower limits on (26) to keep them within a range expected for targets of interest and to mitigate the impact of outliers.

Finally, the estimated RCS is computed to be the weighted average of the short- and long-term estimated RCS values,

$$\hat{\sigma}_{k|k}^i = \hat{\sigma}_{k|k}^{i_1} \cdot p_k(h_1) + \hat{\sigma}_{k|k}^{i_2} \cdot p_k(h_2) \quad (28)$$

When this blended RCS estimate is used to evaluate the likelihood score, the *propagated* version is used when the next frame of data is received. However, without a model for the RCS change with time, the propagated RCS estimate is simply the last updated value, $\hat{\sigma}_{k+1|k}^i \triangleq \hat{\sigma}_{k|k}^i$.

[‡]If we assume the log-normal distribution, then $\hat{\sigma}$ is an estimate of the *median* value of the RCS.

4.2. Modified Two-Model RCS Estimator with Median Filters

A modification of the approach shown in Section 4.1 was developed by replacing the α -filters shown in (26) with median filters. The motivation for doing so was that median filters are known in the statistical community to be a good choice for processing data with significant outliers. RCS distributions such as Swerling I have a significantly large “tail,” thus there is a significant possibility of receiving large RCS measurements relative to the mean RCS.

The filter is implemented by computing the median value of the RCS over the recent w_1 (short) or w_2 (long) windows of measurements,

$$\hat{\sigma}_{k|k}^{i_1} = \text{median} \left(\sigma_{k-w_1+1}^{j_k}, \dots, \sigma_k^{j_k} \right), \quad \hat{\sigma}_{k|k}^{i_2} = \text{median} \left(\sigma_{k-w_2+1}^{j_k}, \dots, \sigma_k^{j_k} \right) \quad (29)$$

These estimators replace the α -filters shown in (26). Notice here that we have augmented the superscript notation such that $\sigma_k^{j_k}$ now specifies some particular measurement j_k on frame k , and this measurement index may be different from the measurement index j_{k-1} on frame $k-1$.

The output estimate of the target RCS is computed using the Bayesian blended RCS as shown in (28). Further, the predicted RCS on frame $k+1$ is also defined by $\hat{\sigma}_{k+1|k}^i \triangleq \hat{\sigma}_{k|k}^i$ since no RCS dynamics model is available.

4.3. IMM Filter RCS Estimator

We present now a new approach to the multiple model RCS estimation problem based on an Interacting Multiple Model (IMM) filter. The IMM technique is well known to be the leading choice in target tracking where multiple “maneuver modes” are present. In the RCS estimation context, a “jump” in the RCS value constitutes a new mode of the RCS state.

4.3.1. Jump-Bias Model IMM Approach

The general idea of the IMM application for RCS tracking is to implement a set of Kalman filters with bias inputs that correspond to possible jump values. Thus, when a large RCS step is experienced, the filter will “switch” to the mode with corresponding bias that best matches the step. Two kinds of filter models can be used: nearly-constant position (NCP), and nearly-constant velocity (NCV). The former is useful when the mean RCS value not changing with time, and the later is useful when the mean RCS is *slowly* varying (rapid changes are handled by the multiple models).

The i th model state equation for the RCS estimation problem is defined as

$$\mathbf{x}_{k+1}^i = \mathbf{F}_k \mathbf{x}_k^i + \mathbf{b}^i + \mathbf{w}_k \quad (30)$$

where \mathbf{x}_k^i and \mathbf{F}_k are discussed below for the cases of NCP and NCV, and $\mathbf{w}_k \sim \mathcal{N}(0, \mathbf{Q}_k)$ is the process noise. The “jump” bias \mathbf{b}^i associated with the i th model is either a vector or scalar depending on whether it is an NCV or NCP model. In the case of the NCV, then it is a vector $\mathbf{b}^i = [b^i, 0]^T$, where b^i is the RCS-mean jump value specified for the i th model. In the case of NCP, then the bias is the mean RCS scalar, $\mathbf{b}^i \triangleq b^i$. By defining a family of jumps $\{b^1, b^2, \dots, b^N\}$, with $b^n = 0$ for some $n \in \{1, \dots, N\}$, then the IMM allows the filter to rapidly transition to RCS steps whenever $i \neq n$ is the best model, and while providing smoothing whenever the model $i = n$ is the best model. Note that the RCS jumps need not match the b^i values since blending of states takes place and “in between” values will result from the combination of two states.

NCV Model. The nearly-constant velocity model has a state that includes RCS and RCS-rate, $\mathbf{x}_k = [\sigma_k, \dot{\sigma}_k]^T$. Thus, the estimate of the mean RCS is extracted as the first component of the state. The RCS-rate can be used for predicting the RCS at a future time, if necessary. The state transition matrix and the process noise matrix are given by

$$\mathbf{F}_k = \begin{bmatrix} 1 & T_k \\ 0 & 1 \end{bmatrix}, \quad \mathbf{Q}_k = q_0 \begin{bmatrix} T_k^3/3 & T_k^2/2 \\ T_k^2/2 & T_k \end{bmatrix} \quad (31)$$

where $T_k = t_{k+1} - t_k$ and q_0 is a user-defined process noise intensity parameter.

NCP Model. The nearly-constant position model has a state that includes only the RCS, $\mathbf{x}_k = \sigma_k$; thus, the state is a scalar. The state transition, $\mathbf{F}_k = 1$, is also a scalar. Likewise, the process noise, $\mathbf{w}_k = q_0 T_k$, is a scalar. Hence, the RCS state equation (30) for the NCP model can be written as

$$\sigma_{k+1}^i = \sigma_k^i + b^i + w_k \quad (32)$$

Note that the level of “smoothing” versus “adaptation to change” in this model can be controlled by the choice of the value of q_0 .

IMM Implementation. The blended IMM output RCS state estimate is computed as

$$\hat{\mathbf{x}}_{k|k} = \sum_{i=1}^N \mu_k^i \hat{\mathbf{x}}_{k|k}^i \quad (33)$$

where μ_k^i is i th mode probability, and where $\hat{\mathbf{x}}_{k|k}^i$ is the Kalman filter state estimate based on the i th model. The RCS estimate $\hat{\sigma}_{k|k}$ is then extracted from $\hat{\mathbf{x}}_{k|k}$. If the IMM configuration includes an NCV filter, then a dynamics model for the RCS is employed and a predicted RCS value $\hat{\sigma}_{k+1|k}$ could be generated from $\hat{\mathbf{x}}_{k+1|k} = \mathbf{F}_k \hat{\mathbf{x}}_{k|k}$. Other details on the IMM filter algorithm implementation are well known and can be found in Ref. 14.

4.3.2. Median Pre-Filter for the IMM Implementation

A unique aspect of the IMM filter implementation for RCS estimation is the application of a median pre-filter. The reason for the pre-filtering is that RCS fluctuation noise, with the large tail distribution, can degrade the performance of the Kalman-based IMM filter. By applying the median pre-filter, outliers are suppressed and the error distribution becomes more log-normal-like. The median pre-filter was successfully used in a glint noise filtering problem.¹⁵ We have not applied the velocity prediction/correction idea developed in Ref. 15 because it is not really needed in this application; the RCS-rate is typically not large and median filter window is short (e.g., $w = 3$).

The pre-filter processing is implemented as follows. If $\sigma_k^{j_k}$ is the j_k th measurement at time t_k , then the output measurement is formed as

$$\tilde{\sigma}_k^j = \text{median} \left(\sigma_{k-w+1}^{j_k}, \dots, \sigma_k^{j_k} \right) \quad (34)$$

where w is the length of the median filter window. The output $\tilde{\sigma}_k^j$ is passed to the IMM filter as the RCS measurement input at time t_k , unless the measurements is exactly the same as $\tilde{\sigma}_{k-1}^j$ (which can happen because the same measurement can be the “median value” on consecutive frames). When the output measurement is identical, then no measurement is passed to the IMM filter (i.e., we coast the filter). This prevents correlation due to repeated measurements from building up in the IMM filter estimates.

It is important to note that the median pre-filter has the effect of changing the input distribution such that the filtered RCS estimates $\hat{\sigma}_{k|k}$ converge to the *median* RCS value. Thus, if one requires the mean value for computation of the likelihood ratio or for RMS accuracy evaluations, the median estimate must be converted to a mean estimate as discussed in Section 3.4.

5. SIMULATION RESULTS

To evaluate the three RCS tracking filters, we constructed two simulation cases that test the ability of the filters to transition over jumps and accurately estimate the RCS.

5.1. Scenario Descriptions and Filter Parameters

Two simulation cases were constructed. Case 1 has static RCS values except for jumps of 10 dBsm and 20 dBsm; the case will show the ability of the filters to transition quickly to new RCS values while still providing smoothing during constant RCS periods. Case 2 consists of slowly varying RCS values with some large jumps. This case will show the ability of the filters to track the RCS and respond to jumps. RCS samples were generated using a Swerling I distribution, with an update rate of 1.0 Hz.

Table 1. Filter parameters for simulation study.

Filter Parameter	Value
α -Filter	
Time constant τ_1	3.0 sec
Time constant τ_2	10.0 sec
Model SDV σ_1	5.0 dBsm
Model SDV σ_2	5.0 dBsm
Min Mode Probability P_{\min}	0.01
Median Filter	
Short Window w_1	3 samples
Long Window w_2	11 samples
Model SDV σ_1	3.0 dBsm
Model SDV σ_2	3.0 dBsm
Min Mode Probability P_{\min}	0.01
IMM Filter	
Median Pre-Filter Window w	3 samples
RCS Measurement Covariance \mathbf{R}	3^2 dBsm ²
Model 1	NCP with $b_1 = -10$ dBsm, $q_0 = 10^0$
Model 2	NCP with $b_2 = 0$ dBsm, $q_0 = 10^0$
Model 3	NCP with $b_3 = 0$ dBsm, $q_0 = 10^{-3}$
Model 4	NCP with $b_4 = +10$ dBsm, $q_0 = 10^0$

The parameters for filters implemented in the simulation study are shown in Table 1. The IMM filter was implemented with four NCP models. Simulations were conducted also with an IMM with three NCP models and one NCV model (the NCV was to track the slowly time varying RCS). However, we found slightly better results using the four NCP models. In the configuration, a central NCP model with $b_i = 0$ and low process noise was to provide the primary smoothing of the mean (median) RCS. Two NCP models with $b_i = \pm 10$ were added to handle the “jumps” in the RCS; a larger family of bias models can be added, depending on the magnitude of target RCS changes and the desired transition rate. A high noise NCP model with $b_i = 0$ was included to handle conditions where the RCS was slowly varying. The following transition matrix was used to encourage transitions to/from the central low-noise NCP model,

$$[p_{ij}] = \begin{bmatrix} 0.90 & 0.05 & 0.05 & 0.00 \\ 0.05 & 0.75 & 0.15 & 0.05 \\ 0.01 & 0.01 & 0.97 & 0.01 \\ 0.00 & 0.05 & 0.05 & 0.90 \end{bmatrix} \quad (35)$$

5.2. Results

Simulation results for case 1 are shown in Figure 1. The results are for 1000 Monte Carlo trials. Plot (a) shows the mean estimated RCS over all runs overlaid on the true mean RCS. Plots (b) and (c) show close-ups of plot (a) at time 50 sec and 200 sec. From these plots we see that the IMM filter has the fastest transition to the steps in mean RCS; the median filter appears to respond nearly as quickly. The α -filter seems to respond the slowest, with a “fading in” of the new value.

Figure 1d shows the RMS value of the RCS estimate over the 1000 trials. Here we see that the IMM filter quickly hits an RCS floor value after jumps. This convergence is expected in IMM filters; inherently, when a small contribution of the “non-matching filter” is mixed into the RCS estimate, it “dilutes” the accuracy. One can mitigate this by adjusting the mixing probabilities (at the expense of other performance factors), or by choosing the “best” matched mode instead of blending all. Such tuning studies could be pursued in the future. Meanwhile, in Figure 1d the median filter accuracy wanes after the 200 sec and 250 sec transitions; during these intervals the short-window median filter dominates, and this leads to lower accuracy. The α -filter accuracy plot shows that it improves after transitions as “smoothing” drives the error down during the flat regions.

Figures 1e through 1g show plots of the mode probabilities for the three filters for case 1. For the IMM, we see that the low-noise NCP filter with $b_3 = 0$ dominates most of the time (red curve), which is the desired response. At the times of the RCS jumps, the bias mode appropriately peaks up; at time 50 sec, the $b_1 = 10$ mode peaks up, at time 200 sec the

$b_4 = -10$ mode peaks up, and at time 250 sec the $b_1 = -10$ mode peaks up. We also see that the high-noise NCP model mode probability peaks up after these transitions; apparently, this filter corrects for some of the inaccuracy in the RCS estimate after the transition. Figure 1f shows the mode probabilities for the median filter. Here, the transitions are more gradual compared to the IMM. Figure 1g shows the mode probabilities for the α -filter; they are similar to the median filter, but the response is even slower. However, one can see from the plots that all three filters properly “detect” RCS jumps and transition to the correct filter mode at the transition point.

Figure 1h shows a plot of the standard deviation of the RMS estimate generated by the IMM filter. Neither the median filter nor the α -filter has the ability to estimate the RMS accuracy of the estimate. The plots shows that the accuracy estimate is slightly optimistic compared to the accuracy shown in Figure 1b. Nevertheless, it correctly follows the error trend. The availability of the RMS estimate is significant in that this estimate could be used in the signal score (e.g., equation (23)) instead of a fixed parameter. This would enable finer tuning of the signal score, and thus better differentiation of targets during the data association process.

Plots for case 2 are shown in Figure 2. In this example, the mean RCS varies with time. We see that all three filters track the RCS reasonably well. The conclusions about the IMM performance are less clear here. In some instances (e.g., time 200 sec) the IMM transitions the fastest of the three filters. In other instances (e.g., 50 sec), the response is comparable to the other two filters. Also, with the time varying nature of the mean RCS, one would expect the high-noise NCP mode (model 2) to provide a higher contribution. A variety of mode transition probabilities and process noise (q_0) values were tried, but the low-noise NCP filter with $b_3 = 0$ typically dominates in this example. It is possible other tunings of the IMM configuration would provide superior filter performance.

6. SUMMARY

In this paper, we presented a methodology for using radar signal features (SNR and RCS measurements from a narrowband radar) for augmenting the track score used in the data association problem. Two main components to the methodology were the signal score likelihood ratio formulation (Section 3), and the multiple model RCS tracking technique to estimate the mean RCS associated with an object (Section 4). Signal scores were derived for three different target fluctuation models: Swerling I, Swerling III, and log-normal. In each of these cases, an estimate of the mean target SNR (or RCS) is needed. The estimate is derived from the RCS tracking filter. Three different tracking filter options were developed: IMM filter, median filter, and α -filter (all using multiple models). A simulation study was performed to compare the RCS tracking filters that showed the following:

- All three RCS filters provide the appropriate tracking performance: they transition when large jumps occur, and they provide smoothing when the RCS is relatively constant.
- The IMM filter provides fast transition to new values after jumps. The median filter also typically provides a fast transition after a jump. The α -filter typically transitions slightly more slowly because it “fades in” the values after a change.
- In terms of RMS accuracy, the α -filter is superior because of the “smoothing” property during periods of near-constant RCS. The IMM filter can provide reasonable accuracy, however, because of the mixing of mis-matched models there is limit to its accuracy performance; techniques to improve the accuracy are available.
- The mode probabilities of all three filters exhibit the expected response to jumps in the mean RCS. In some applications, it could be useful to monitor these mode probabilities to detect changing conditions.
- The IMM filter is able to generate an estimate of the RMS accuracy of the filter (from the state covariance). This is useful for computing the signal score and may provide a significant “tuning capability” relative to the other two filter methods.

In future work, the RCS tracking filter and the signal score methodology will be integrated into the tracking filter and tested in closely-spaced object scenarios. This will enable the value of the feature-aided tracking to be assessed.

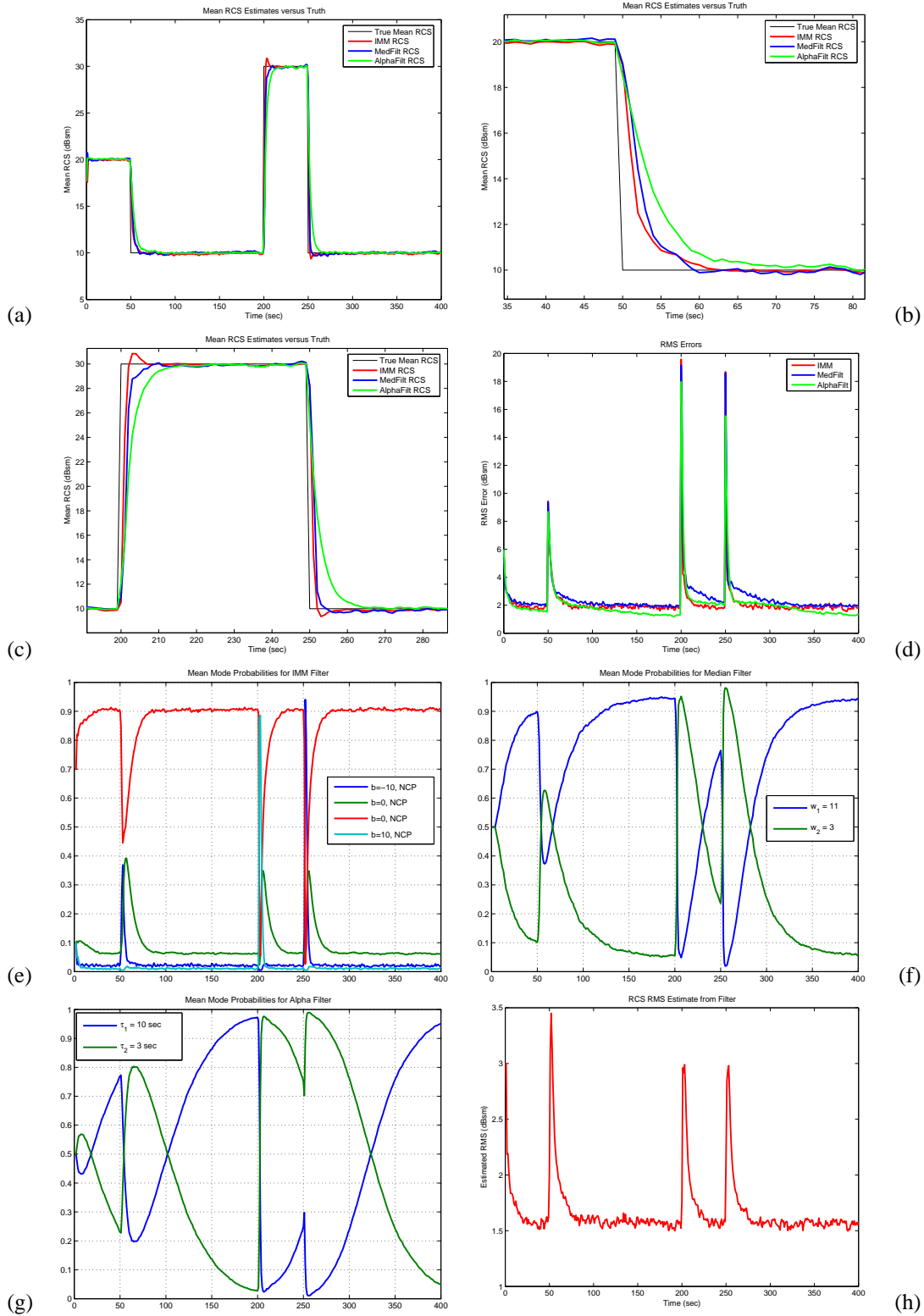


Figure 1. Plots for case 1: (a) mean RCS estimate, (b) close up of mean RCS at 50 sec, (c) close up of mean RCS at 200 sec, (d) RMS of the estimate, (e) IMM mode probabilities, (f) median filter mode probabilities, (g) α -filter mode probabilities, (h) IMM filter estimate of RMS.

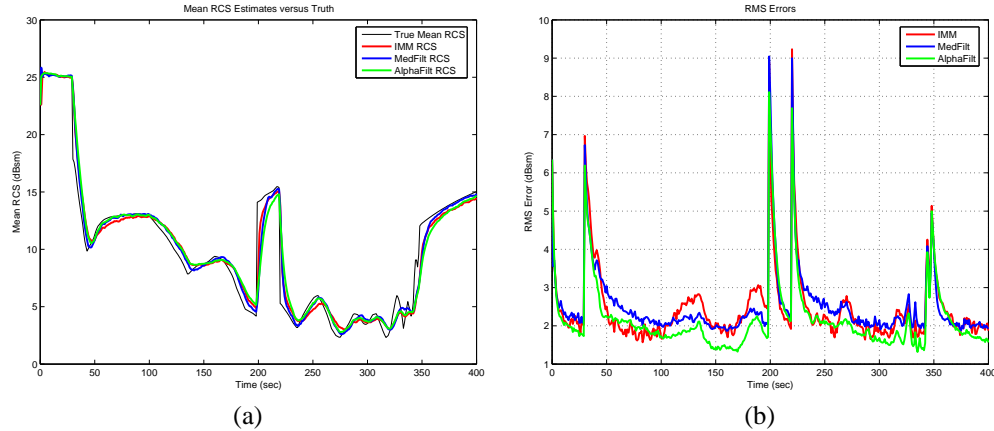


Figure 2. Plots for case 2: (a) mean RCS estimate, (b) RMS of the estimate.

ACKNOWLEDGMENTS

The authors acknowledge the helpful conversations and contributions of Sam Blackman to this paper. This work was supported in part by the US Army under contract W9113M-05-C-0086.

REFERENCES

1. O. E. Drummond, "Feature, attribute, and classification aided target tracking," in *Proceedings of SPIE, Conference on Signal and Data Processing of Small Targets*, **4473**, pp. 542–558, 2001.
2. O. E. Drummond, "Attribute in tracking and classification with incomplete data," in *Proceedings of SPIE, Conference on Signal and Data Processing of Small Targets*, **5428**, pp. 476–496, April 2004.
3. D. Lerro and Y. Bar-Shalom, "Interacting multiple model tracking with target amplitude feature," *IEEE Transaction on Aerospace and Electronic Systems* **29**, pp. 494–509, April 1993.
4. P. F. Singer and A. L. Coursey, "Feature aided tracking (FAT)," in *Proceedings of SPIE, Conference on Signal and Data Processing of Small Targets*, **5428**, pp. 249–259, 2004.
5. C. S. Agate and K. J. Sullivan, "Signature-aided tracking using association hypotheses," in *Proceedings of SPIE, Conference on Signal Processing, Sensor Fusion, and Target Recognition XI*, **4729**, pp. 44–55, 2002.
6. D. H. Nguyen, J. H. Kay, B. J. Orchard, and R. H. Whiting, "Feature-aided tracking of moving ground vehicles," in *Proceedings of SPIE, Conference on Algorithms for Synthetic Aperture Radar Imagery IX*, **4727**, 2002.
7. J. Lancaster, S. Blackman, and E. Taniguchi, "Joint IMM/MHT tracking and identification with application to ground targets," in *Proceedings of SPIE, Conference on Signal and Data Processing of Small Targets*, **5913**, August 2005.
8. S. Blackman and R. Popoli, *Design and Analysis of Modern Tracking Systems*, Artech House, Norwood, MA, 1999.
9. S. S. Blackman and R. Dempster, "Description of the UEWB MHT tracker (revised)," technical report, Raytheon Corporation, RE/R07/P572, PO Box 902, El Segundo, CA 90245, 2002.
10. P. Swerling, "Probability of detection for fluctuating targets," Technical Report RM-1217, Rand Corporation, March 17, 1954.
11. M. I. Skolnik, *Introduction to Radar Systems*, McGraw Hill, Boston, MA, 3 ed., 2001.
12. P. R. Runkle, P. K. Bharadwaj, L. Couchman, and L. Carin, "Hidden Markov models for multiaspect target classification," *IEEE Transactions on Signal Processing* **47**, pp. 2035–2040, July 1999.
13. P. L. Ainsleigh, N. Kehtarnavaz, and R. L. Streit, "Hidden Gauss-Markov models for signal classification," *IEEE Transactions on Signal Processing* **60**, pp. 1355–1367, June 2002.
14. Y. Bar-Shalom, X. R. Li, and T. Kirubarajan, *Estimation with Applications to Tracking and Navigation*, John Wiley & Sons, Inc., New York, 2001.
15. D. C. Chang and W. R. Wu, "Feedback median filter for robust preprocessing of glint noise," *IEEE Transactions on Aerospace and Electronic Systems* **36**, pp. 1026–1035, October 2000.